

AH23848 accelerates inducible nitric oxide synthase degradation through attenuation of cAMP signaling in glomerular mesangial cells

Yu-Sheng Lin ^{a,c}, Mingli Hsieh ^b, Yi-Ju Lee ^c, Kai-Li Liu ^d, Ting-Hui Lin ^{e,*}

^a Institute of Oral Medicine, Chung Shan Medical University, No. 110 Jianguo North Road, Section 1, Taichung 40203, Taiwan, ROC

^b Department of Life Science, Tunghai University, Box 851, No. 181, Section 3, Taichung-Kan Road, Taichung 40704, Taiwan, ROC

^c Institute of Immunology, Chung Shan Medical University, No. 110 Jianguo North Road, Section 1, Taichung 40203, Taiwan, ROC

^d Department of Nutrition, Chung Shan Medical University, No. 110 Jianguo North Road, Section 1, Taichung 40203, Taiwan, ROC

^e Department of Biomedical Sciences, Chung Shan Medical University, No. 110 Jianguo North Road, Section 1, Taichung 40203, Taiwan, ROC

Received 7 August 2007; revised 23 October 2007

Available online 6 November 2007

Abstract

Excessive release of nitric oxide (NO) by mesangial cells contributes to the pathogenesis of glomerulonephritis. Prostaglandin E₂ (PGE₂) produced at inflammatory sites regulates the release of NO through its downstream signaling. In glomerular mesangial cells (MES-13 cells), PGE₂ modulated NO production mainly through EP4 receptor in a cAMP-dependent manner. Lipopolysaccharide and interferon- γ (LPS + IFN γ)-induced NO production, inducible nitric oxide synthase (iNOS) gene and protein expression were greatly inhibited by AH23848, an EP4 antagonist. Further investigation indicated that AH23848 attenuated endogenous cAMP accumulation in MES-13 cells and modulated NO production through declination of iNOS gene expression and acceleration of iNOS protein degradation. AH23848 downregulated the iNOS protein in MES-13 cells through protein kinase A (PKA) since KT5720, a PKA-specific inhibitor, reduced iNOS protein stability. A short exposure of activated MES-13 cells to okadaic acid augmented iNOS activity. AH23848 and KT5720 attenuated serine/threonine phosphorylation of iNOS protein in LPS + IFN γ -stimulated MES-13 cells. The results of this study led us to speculate that cAMP might regulate iNOS-stimulated NO synthesis through posttranslational mechanisms. Attenuation of cAMP signaling and the phosphorylation status of the iNOS protein may account for the effect of AH23848 in accelerating iNOS protein degradation in MES-13 cells.

© 2007 Elsevier Inc. All rights reserved.

Keywords: Prostaglandin E₂; AH23848; cAMP; Inducible nitric oxide synthase; Protein degradation; Glomerular mesangial cells

An increase in the production of nitric oxide (NO)¹ with the development of glomerulonephritis has been demonstrated [1]. NO, a messenger gas generated from L-argi-

nine, is the product of nitric oxide synthase (NOS). NO balances the glomerular microvascular tone when produced in low amounts. During inflammation, excess yields of NO as a result of inducible NOS (iNOS) activation cause cytotoxicity [2]. Overproduction of NO in response to lipopolysaccharide (LPS) or cytokines leads to renal damage and contributes to the pathogenesis of glomerulonephritis [2]. In the present study, MES-13 cells, an SV-40-transformed mouse mesangial cell line which maintains its ability to express iNOS in response to LPS and cytokines, were used to investigate the effects of prostaglandin E₂ (PGE₂), another important immune mediator, on iNOS-stimulated NO production and their roles in glomerulonephritis.

* Corresponding author. Fax: +886 4 2475 7412.

E-mail address: thlin@csmu.edu.tw (T.-H. Lin).

¹ Abbreviations used: Buta, butaprost; COX-2, cyclooxygenase 2; FK, forskolin; IBMX, isobutylmethylxanthine; IFN- γ , interferon- γ ; iNOS, inducible nitric oxide synthase; LPS, lipopolysaccharide; MES-13 cells, mouse glomerular mesangial cells; NO, nitric oxide; PCR, polymerase chain reaction; PI 3-K, phosphatidylinositol 3-kinase; PKA, protein kinase A; PGE₂, prostaglandin E₂; PSAb, a phospho-(serine/threonine) PKA substrate antibody; PVDF membrane, polyvinylidene difluoride membrane; Sulp, sulprostone; TBS, tris-buffered saline; TBST, tris-buffered saline containing Tween 20; 11-D, 11-deoxy PGE₁; 17-P, 17-phenyl trinor PGE₂.

PGE₂, the most prevalent derivative of arachidonic acid, modulates cellular and humoral immune responses [3]. With respect to iNOS-stimulated NO production, PGE₂ exhibits biphasic effects in a cell type-specific manner [4]. The mechanism underlying this differential effect remains unclear, but may be attributed to the complexity of PGE₂ receptors and their downstream signaling pathways [5]. At least four subtypes of PGE₂ receptors (EP1, EP2, EP3, and EP4) have been identified [5]. Through activation of Ca²⁺/inositol phospholipid via EP1 receptors, PGE₂ negatively regulated iNOS induction [6], while PGE₂ upregulated NO production via a cAMP-dependent protein kinase pathway in rat mesangial cells and murine breast cancer cells, respectively [7,8].

Similar to the paradoxical effects of PGE₂ on iNOS-stimulated NO production, contradictory effects of cAMP on iNOS activity have been demonstrated in a variety of cells. cAMP has been shown to regulate the expression of iNOS through either stimulatory or inhibitory effects [9]. The mechanism involved in the differential effects of cAMP on iNOS expression is intricate. The best-known action of cAMP on regulation of iNOS expression is mainly controlled at the transcriptional level. Binding of cAMP to protein kinase A (PKA) releases the catalytic subunits of PKA. Active PKA then phosphorylates and activates transcriptional factors which bind to the promoter/enhancer region of the iNOS gene [10]. Whether cAMP exerts positive or negative effects on iNOS depends on specific transcription factors activated in certain cells [10] or through modulation of the endogenous cytokine network [11]. Recently, Won et al. [9] reported that cAMP regulated iNOS expression at the posttranslational level in macrophages. Forskolin (FK) increased iNOS stability via inhibition of ubiquitination of iNOS protein in RAW264.7 macrophages. A potential role of cAMP in protecting iNOS from degradation is thus indicated.

Diverse factors including dexamethasone and transforming growth factor-β1 attenuate iNOS-stimulated NO production through enhanced iNOS protein degradation [12,13]. iNOS is targeted for degradation either through proteasome or calpain I pathways [14,15]. Ubiquitination of iNOS and the subsequent degradation of the iNOS protein by proteasomes have been shown in murine RAW 264.7 macrophages [14]. Proteolytic cleavage of iNOS by calpain I requires a correct conformation determined by calmodulin-binding domains within the iNOS protein [15]. Moreover, degradation of NOS proteins is modulated through interactions with proteins. In human intestinal carcinoma HT29 and DLD1 cells, overexpression of caveolin-1 promotes degradation of iNOS via the proteasome pathway [16]. Heat-shock protein 90 acts as a protector of iNOS by increasing its protein half-life [17,18]. Thus, the mechanism involving iNOS degradation is complex. Whether a cAMP-dependent PKA pathway modulates iNOS protein degradation is unclear.

In the present study, the presence of the EP4 receptor for PGE₂ and its downstream signaling in MES-13 cells

were elucidated. Exogenous addition of PGE₂ or 11-deoxy PGE₂ slightly enhanced LPS + IFNγ-induced NO production, while AH23848, an EP4 antagonist, significantly suppressed LPS + IFNγ-induced NO production in MES-13 cells. Through attenuation of endogenous cAMP accumulation and a reduction in PKA signaling, AH23848 inhibited NO production via diminishing iNOS gene expression and accelerating iNOS protein degradation in MES-13 cells.

Materials and methods

Materials

PGE₂, 17-phenyl trinor PGE₂, butaprost, 11-deoxy PGE₁, and sulprostone were obtained from Cayman Chemical Company (Ann Arbor, MI, USA). Fetal bovine serum (FBS) and trypsin were purchased from Hyclone (Logan, UT, USA). Recombinant mouse IFNγ was provided by PeproTech EC (London, UK). LPS and FK were purchased from Sigma Chemical Company (St. Louis, MO, USA). Cell culture reagents were from Life Technologies (Gaithersburg, MD, USA). The anti-iNOS antibody was purchased from Santa Cruz Biotechnology, Inc. (Santa Cruz, CA, USA). The phospho-(serine/threonine) PKA substrate antibody (PSAb) was purchased from Cell Signaling Technology (Beverly, MA, USA). Redivue™ L-[³⁵S] methionine (>370 MBq/ml; 10 mCi/ml) and [¹⁴C] arginine monohydrochloride (>300 mCi/mmol; 50 mCi/ml) were purchased from Amersham International (Buchs, UK). All other chemicals were reagent grade.

Cell culture

The MES-13 cell line (glomerular mesangial cells from an SV40 transgenic mouse) was obtained from American Type Culture Collection (CRL-1927; Manassas, VA, USA) and maintained in culture medium with a 3:1 mixture of Dulbecco's modified Eagle's medium (DMEM) and Ham's F12 medium, supplemented with 14 mM Hepes, 2 mM glutamine, antibiotics (100 μg/ml penicillin and 100 μg/ml streptomycin), and 5% fetal bovine serum at 37 °C. The incubation chamber was equilibrated with 5% CO₂-95% air.

Reverse-transcriptase polymerase chain reaction (RT-PCR)

Total RNA was isolated from MES-13 cells using the Tri reagent RNA isolation reagent (Molecular Research Center, Inc., Cincinnati, OH, USA). First-strand cDNA was prepared with an oligo-dT primer and Superscript II reverse transcriptase (Life Technologies, Gaithersburg, MD, USA) from MES-13 cell RNA and subsequently amplified in a polymerase chain reaction (PCR). The primers for four PGE₂ receptors were selected from the sequences reported by Nasrallah et al. [19]. The primers for iNOS were designed according to the procedures of Cheng et al. [20]. The sequences of primers for the RT-PCR and the expected length of PCR products were as follows: the EP1 receptor (336 bp): 5'-CGCAGGGTTCACGCACA CGA-3' and 5'-CACTGTGCCGGGAACATACGC-3'; the EP2 receptor (401 bp): 5'-AGGACTTCGATGGCAGAGGAGAC-3' and 5'-CAGCC CCTACTTCTCCAATG-3'; the EP3 receptor (437 bp): 5'-CCGGGC ACGTGGTGTTCAT-3' and 5'-TAGCAGCAGATAAACCCAGG-3'; the EP4 receptor (423 bp): 5'-TTCCGCTCGTGGTGGCAGTGTTC-3'; and iNOS (353 bp): 5'-CAGTTCTGCGCCTTTGCTCAT-3' and 5'-GGT GGTGCGGCTGGACTT T-3'. DNA amplification was carried out in a solution containing 1× AmpliTaq Gold buffer, 1.5 mM MgCl₂, 0.5 μM of the desired primers, 0.2 mM of each deoxynucleoside triphosphate (dNTP), 1 μl cDNA template, and 2.5 units of AmpliTaq Gold DNA polymerase per 50 μl of reaction solution. To confirm that the PCR products were really PGE₂ receptors, the PCR-amplified DNA fragments were eluted

from the gel and subcloned into a pGEM-T Easy Vector system (Promega, Madison, WI, USA). After blue/white selection, the white colonies were picked out and then sequenced using dideoxynucleotide chain termination.

Cyclic AMP assay

Cells were cultured in 6-well plates to about 80% confluency (approximately 1.2×10^5 cells/well) and washed twice with $1 \times$ PBS. Prior to stimulation, cells were preincubated for 10 min at 37°C in medium containing 0.5 mM isobutylmethylxanthine (IBMX). The individual agonists and antagonists for each receptor were added to the medium containing 0.5 mM IBMX. Cells were then incubated at 37°C for 10 min. The reaction was terminated by the rapid removal of medium. Cell lysis and extraction of cAMP were performed by the addition of 65% ice-cold ethanol and incubation on ice. The amount of cAMP extracted from each well was quantified by a cAMP Biotrak enzyme immunoassay (EIA) system (Amersham Biosciences, Piscataway, NJ, USA).

Intracellular calcium measurements

To investigate the signaling pathway of the EP1 receptor, the effect of PGE₂ on intracellular Ca²⁺ mobilization of MES-13 cells was measured. MES-13 cells were cultured on 3.5-mm coverslips the day before the calcium measurement. The culture medium was removed, and the cells were maintained in Hepes-phosphate buffer containing (in mM) 140 NaCl, 5.4 KCl, 1.26 CaCl₂, 0.5 MgCl₂, 0.4 MgSO₄, 0.34 Na₂HPO₄, 0.44 KH₂PO₄, 10 Hepes, and 10 glucose (pH, 7.4). A stock solution of 1 mM Ca²⁺-sensitive dye (fluo-3 acetoxymethyl ester; Fluo-3/AM) (Molecular Probes, Eugene, OR, USA) was dissolved in DMSO and diluted to a final 3–5 μM with Hepes-phosphate buffer. The dye solution was loaded onto MES-13 cells on a coverslip for 40–60 min at room temperature in the dark. Cells loaded with fluo-3-AM were quantified by an inverted confocal laser-scanning microscope (Zeiss Axiovert 135 M, Germany), with excitation at 488 nm and emission at 525 nm. Changes in intracellular calcium levels of MES-13 cells were indicated by the relative Fluo-3 fluorescence intensity. Scanned pictures were recorded in a computer by LSM 410 software at 10-s intervals before and after the addition of 10^{-6} M PGE₂. Fluorescent images were converted to a gray scale for analysis using LSM 410 software or Scion (NIH) software.

Nitrite assay

Nitrite assay was performed to measure NO production in MES-13 cells after different treatment. Nitric oxide (NO) is rapidly converted into nitrite as the end product. Thus, the nitrite accumulation in culture supernatant was used as indirect measures of the amount of NO produced. The Griess assay was used and the nitrite level was measured in triplicate. Briefly, an aliquot of 100 μl of the culture supernatant of MES-13 cells was mixed with 100 μl of Griess reagent (one part 0.1% *N*-(1-naphthyl)ethylene-diamine dihydrochloride in water and one part 1% sulfanilamide in 5% H₃PO₄; both purchased from Sigma Chemicals). The mixture was incubated for ten minutes at room temperature in the dark. The absorbance at 540 nm was measured and the nitrite concentration was calculated by comparison to standard curves of sodium nitrite in culture medium.

Northern blot analysis

To detect the mRNA levels of iNOS in MES-13 cells after exposure to different stimuli, Northern blot analysis was performed. Total cellular RNA was extracted from MES-13 cells using Tri reagent (Molecular Research Center, Inc. Cincinnati, OH, USA) according to the manufacturer's instructions. RNA samples (20 μg) were fractionated on 1% agarose gels containing formaldehyde and then transferred to nylon membranes. The membranes were hybridized with a ³²P-labeled probe for 18 h. The probe was prepared from an RT-PCR product of the iNOS gene according to the primers designed above. After hybridization, the

membrane was washed twice with a solution containing 150 mM NaCl, 15 mM sodium citrate, and 0.1% SDS at 65°C , and then exposed to Kodak X-ray film for 3 days at -80°C with one intensifying screen. Potential loading differences between lanes were corrected by normalizing the RNA amount of each sample, using 28S ribosomal RNA as an internal control. The hybridization signal was quantified by densitometric analysis with Zero-Dscan.

Western blot analysis

To detect the protein levels of iNOS after exposure to different stimuli, MES-13 cells were washed with $1 \times$ PBS, scraped out, then treated with lysis buffer. The lysis buffer contained $1 \times$ PBS, 1% Nonidet P-40, 0.5% sodium deoxycholate, and 0.1% SDS. Protease inhibitors including 1 mM phenylmethylsulfonyl fluoride, 0.15 U/ml aprotinin, and 1 mM sodium orthovanadate were included in the lysis buffer. Cells suspended in lysis buffer were sonicated. The homogenate was centrifuged at 15,000 rpm for 30 min at 4°C , and the cell supernatant was collected. The protein concentration was measured using a Bio-Rad protein assay kit. Cell lysate was combined with $5 \times$ sample buffer containing 100 mM Tris-HCl (pH 6.8), 20% glycerol, 7% SDS, 5% mercaptoethanol, and 0.1% bromophenol blue. The sample was boiled for 5 min and centrifuged to remove the debris. Equal amounts of protein samples (30 μg) were subjected to SDS-PAGE using 7.5% polyacrylamide gels. Following electrophoresis, the gel was transferred to a polyvinylidene difluoride (PVDF) membrane, blocked with 5% skim-milk in Tris-buffered saline (TBS) containing 10 mM Tris (pH 8.0) and 150 mM NaCl, then incubated with iNOS antibody at 4°C overnight. TBS containing 0.02% Tween 20 (TBST) was used to wash out the nonspecific binding material on the PVDF membrane. Finally, the membrane was incubated with secondary antibody for 1 h at room temperature. After washing with TBST, the immunoreactive bands were visualized with a light-emitting kit (ECL, Amersham, UK). The protein amount was quantified by measuring the area of the iNOS protein band using densitometric analysis with Zero-Dscan.

Immunoprecipitation

Total protein (6 mg) collected from the cell lysate was dissolved in 500 μl RIPA buffer containing $1 \times$ PBS, 1% Nonidet P-40, 0.5% sodium deoxycholate, 0.1% SDS, and protease inhibitors including 1 mM PMSF, 0.15 U/ml aprotinin, and 1 mM sodium orthovanadate. Total cellular proteins were then mixed with 10 μl (2 μg) of an iNOS antibody linked to 2.5 mg Protein A-Sepharose beads with gentle agitation at 4°C for 2 h. The mixture was briefly spun down, and the pellet was washed three times with ice-cold RIPA buffer. Samples were resuspended in $5 \times$ sample buffer containing 100 mM Tris-HCl (pH 6.8), 20% glycerol, 7% SDS, 5% mercaptoethanol, and 0.1% bromophenol blue, boiled at 95°C for 5 min, and analyzed by Western blot analysis.

Measurement of iNOS activity

MES-13 cells with different stimuli were collected in extraction buffer containing 50 mM Tris-HCl (pH 7.5), 0.1 mM EDTA, 10 $\mu\text{g/ml}$ leupeptin, and 1 mM PMSF. Extracted cells were sonicated and centrifuged at 15,000 rpm for 30 min at 4°C . The total protein amount (around 0.2 mg) was incubated at 37°C for 20 min with assay buffer containing 50 mM Tris-HCl (pH 7.5), 1 mM NADPH, 10 μM arginine, 100 μM NaBH₄, and 0.1 $\mu\text{Ci/ml}$ L-[¹⁴C] arginine monohydrochloride. The reaction was terminated by the addition of 1 ml stop buffer containing 20 mM HEPES (pH 5.5) and 2 mM EDTA. The mixture (1.1 ml) was immediately transferred to a 1-ml Dowex 50 W-X8-400 (Aldrich) column. Following the addition of 1 mM citrulline, L-[³H] citrulline in the eluate was quantified by liquid scintillation counting, and iNOS activities were calculated as the formation of L-[³H]-citrulline/min/mg of protein. Measurement of

iNOS activity was used to detect whether inhibitors of serine/threonine protein kinases and tyrosine protein kinases modulates iNOS activity in MES-13 cells.

Determination of iNOS stability

To determine the iNOS protein stability, a pulse-chase study was performed. MES-13 cells were cultured and incubated with 1 µg/ml LPS + 5 ng/ml IFN γ alone or addition with either 30 µM AH23848 or 1 µM KT5720 for 18 h. The culture medium was then removed and replaced with starvation medium containing no methionine for 45 min. Pulse medium containing L-[35 S] methionine (100 µCi per dish) was incubated with cells for 3 h followed by chase medium containing no labeled methionine. The cell lysate was then collected at the indicated time points (1, 3, and 6 h) and labeled iNOS protein was detected by immunoprecipitation, SDS-PAGE, and autoradiography. The protein amount was quantified by measuring the area of iNOS protein band using densitometric analysis with Zero-Dscan.

Statistical analysis

The NO data are means \pm SEM values of three separate experiments, each done in triplicate. cAMP values are means \pm SD of triplicate assays from a representative of two similar experiments. Statistical analysis was performed by Student's *t*-test and a *p* value of <0.05 was considered statistically significant.

Results

Distribution of PGE $_2$ receptor mRNA in MES-13 cells

RT-PCR was used to identify the major PGE $_2$ receptors in MES-13 cells. Using RT-PCR, we were able to detect mRNAs coded for the EP1, EP2, EP3, and EP4 receptors in the kidney (Fig. 1a). mRNAs for EP1, EP2, and EP4 (Fig. 1a-A, B, and D) were detected, whereas mRNAs for EP3 (Fig. 1a-C) were not detected in MES-13 cells. After sequencing the eluted PCR product, the distribution of all EP1, EP2, and EP4 receptors was confirmed in this cell line.

Effect of specific PGE $_2$ agonists on cAMP accumulation in MES-13 cells

To determine potential involvement of the cAMP signaling pathway in PGE $_2$, the response of cAMP to specific agonists for PGE $_2$ receptors was measured in MES-13 cells. The level of cAMP of non-treated MES-13 cells (i.e., the control) was 207 ± 25 fmol/well containing 1.2×10^5 cells (Fig. 1b). The addition of PGE $_2$ (10^{-6} M) increased the cAMP level to 3180 ± 34 fmol/well, which was approximately 15-fold higher than that of the control. Butaprost, a selective EP2 agonist slightly altered the cAMP level (338 ± 21 fmol/well), whereas 11-deoxy-PGE $_1$, an agonist for both EP2 and EP4, markedly increased cAMP to 2194 ± 99 fmol/well. 17-Phenyl trinor PGE $_2$ and sulprostone, specific agonists for EP1 and EP3, respectively, produced little change in cAMP levels (386 ± 17 and 366 ± 16 fmol/well, respectively). Apparently, EP4 is the main receptor subtype responsible for cAMP production

in MES-13 cells. The results suggest that the increase in cAMP potency was the highest with PGE $_2$ followed in decreasing order by 11-deoxy PGE $_1$ and the other PGE $_2$ agonists (Fig. 1b). To determine whether PGE $_2$ affect intracellular calcium in MES-13 cells through EP1, the effects of ionomycin, PGE $_2$ and 17-phenyl trinor PGE $_2$ on intracellular Ca $^{2+}$ mobilization of MES-13 cells were measured. Ionomycin, a calcium ionophore, rapidly increased intracellular calcium in MES-13 cells (data not shown). Addition of either PGE $_2$ or 17-phenyl trinor PGE $_2$ had no effect on intracellular calcium in MES-13 cells (data not shown).

Effects of PGE $_2$ agonists, antagonists and the COX-2 inhibitor on LPS + IFN γ -induced NO production, iNOS mRNA and protein expressions in MES-13 cells

NO production in the presence of test compounds was measured in MES-13 cells. The combination of 1 µg/ml LPS + 5 ng/ml IFN γ showed a significant increase in NO production after 18 h of incubation (6.4 ± 0.14 vs. 1.34 ± 0.11 µmol/L of the control) (Fig. 2a). Effects of specific PGE $_2$ agonists on NO production in MES-13 cells were determined as shown in Fig. 2a. The addition of 10^{-6} M PGE $_2$ into the LPS + IFN γ mixture slightly enhanced NO production to 7.38 ± 0.06 µmol/L. Moreover, the addition of 10^{-6} M 11-deoxy PGE $_1$ to the LPS + IFN γ mixture stimulated NO production to 7.45 ± 0.09 µmol/L. On the contrary, at 10^{-6} M, neither 17-phenyl trinor PGE $_2$, butaprost, nor sulprostone showed any effect on NO production. To confirm the roles of different EP receptors in endogenous PGE $_2$ -mediated NO production, the effects of selective antagonists of PGE $_2$ receptors on NO production were determined. The addition of 10 µM SC19220 (an EP1 antagonist) and 10 µM AH6809 (an EP2 antagonist) showed no effect on NO production, while 10 µM AH23848, an EP4 antagonist, significantly attenuated NO production from 6.4 ± 0.14 to 5.5 ± 0.18 µmol/L (Fig. 2b). Moreover, the NO concentration in the medium was measured in the presence of NS-398, a selective cyclooxygenase 2 (COX-2) inhibitor. NS-398 at 10 µM significantly reduced the LPS + IFN γ -induced NO production from 6.4 ± 0.14 to 3.23 ± 0.15 µmol/L. The extent of NO inhibition in the presence of the COX-2 inhibitor was close to the effect of 30 µM AH23848, which reduced the LPS + IFN γ -induced NO production from 6.4 ± 0.14 to 3.48 ± 0.91 µmol/L (Fig. 3a). Effects of the EP4 agonists and antagonists, and a COX-2 inhibitor on iNOS mRNA were measured. As shown in Fig. 3b, the expression of iNOS mRNA was significantly induced with the addition of LPS + IFN γ , but insignificant enhancement of mRNA was observed with further addition of either PGE $_2$ or 11-deoxy PGE $_1$. Conversely, addition of AH23848 and NS-398 to the LPS + IFN γ mixture markedly attenuated iNOS mRNA expression (Fig. 3b). Further investigation of the effect of EP4 agonists and antagonists, and the COX-2 inhibitor

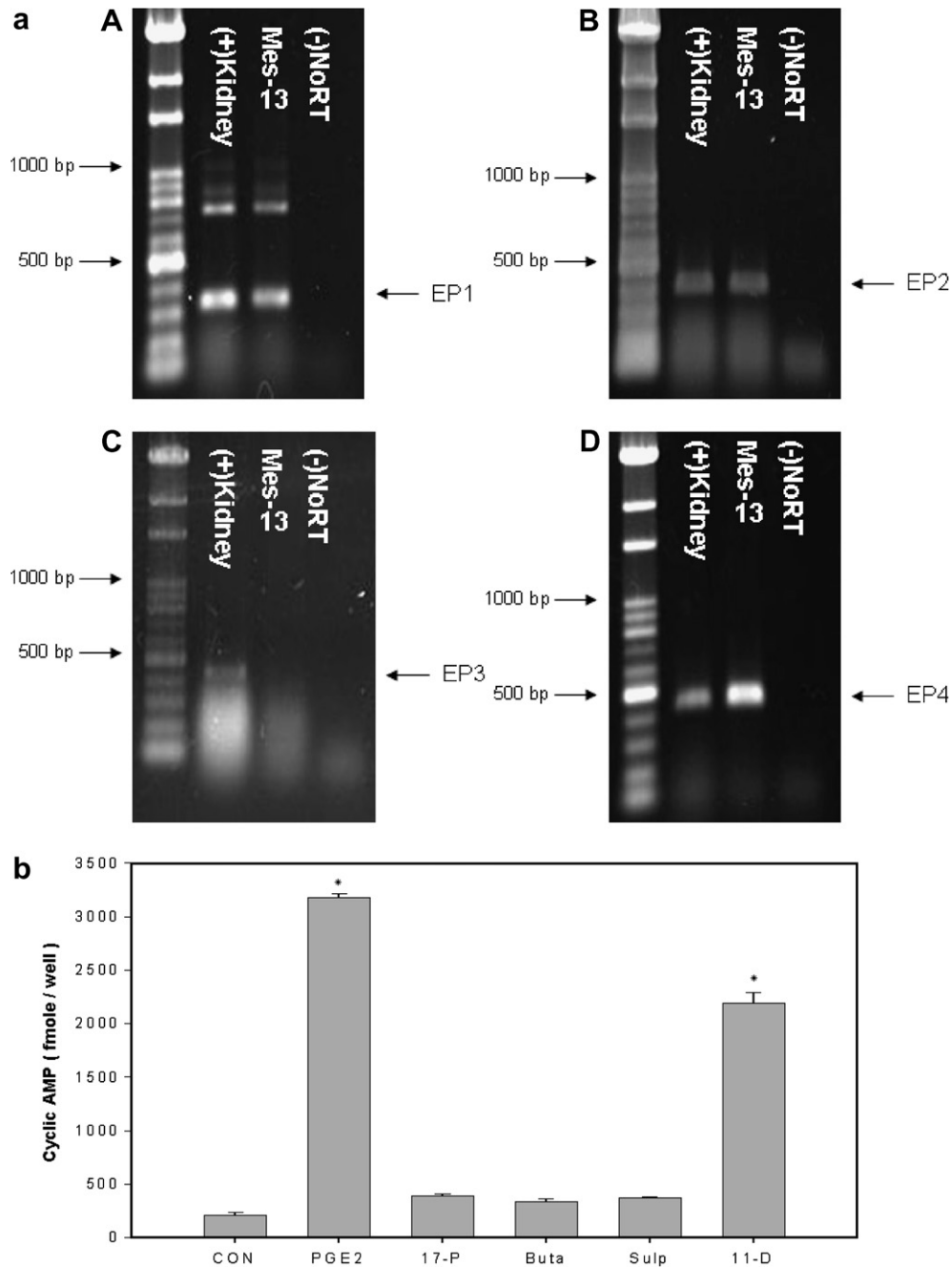


Fig. 1. (a) Distribution of PGE₂ receptor mRNA in MES-13 cells. Total RNA prepared by a tri-reagent was used to detect mRNA coded for EP1, EP2, EP3, and EP4 by RT-PCR. The sequences of the PCR-amplified fragments were further analyzed as described in Materials and methods. (A–D) RT-PCR amplifications of EP1, EP2, EP3, and EP3, respectively, in RNA extracts of mouse kidney and MES-13 cells. As shown in (A), two PCR fragments (336 and 700 bp) were amplified in MES-13 cells. When EP1-specific primers were used in the RT-PCR, the size of 336 bp was confirmed to be EP1 as revealed by DNA sequencing. (–) No RT, a negative control determined in the absence of reverse transcriptase. As shown in (B) and (D), EP2 and EP4 were present in MES-13 cells. On the other hand, EP3 was undetectable in MES-13 cells as shown in (C). (b) Effect of specific PGE₂ agonists on cAMP accumulation in MES-13 cells. Prior to stimulation, cells (approximately 1.2×10^5 cells/well) were preincubated for 10 min at 37 °C in medium containing 0.5 mM IBMX. The individual agonists for each receptor were added to the medium containing 0.5 mM IBMX. Cells were then incubated at 37 °C for 10 min. The amount of cAMP extracted from each well was quantified by the cAMP Biotrak enzyme immunoassay (EIA) system. The cAMP values are means \pm SD of triplicate assays from a representative of two similar experiments. **p* < 0.05 compared to untreated MES-13 cells. CON, control; 11-D, 11-deoxy- PGE₁; Buta, butaprost; Sulp, sulprostone; 17-P, 17-phenyl trinor PGE₂.

on iNOS protein was performed. LPS + IFN γ induced the relative amount of iNOS protein in MES-13 cells. Again, co-supplementation of LPS + IFN γ with PGE₂ or 11-deoxy PGE₁ only slightly enhanced iNOS protein amount (Fig. 3c). On the other hand, addition of AH23848 and

NS-398 to the LPS + IFN γ mixture markedly attenuated 50% of iNOS protein amount. These data indicated that exogenous PGE₂ vaguely enhanced NO production and iNOS protein expression, while blocking endogenous PGE₂ with either an EP4 antagonist or a COX-2-specific

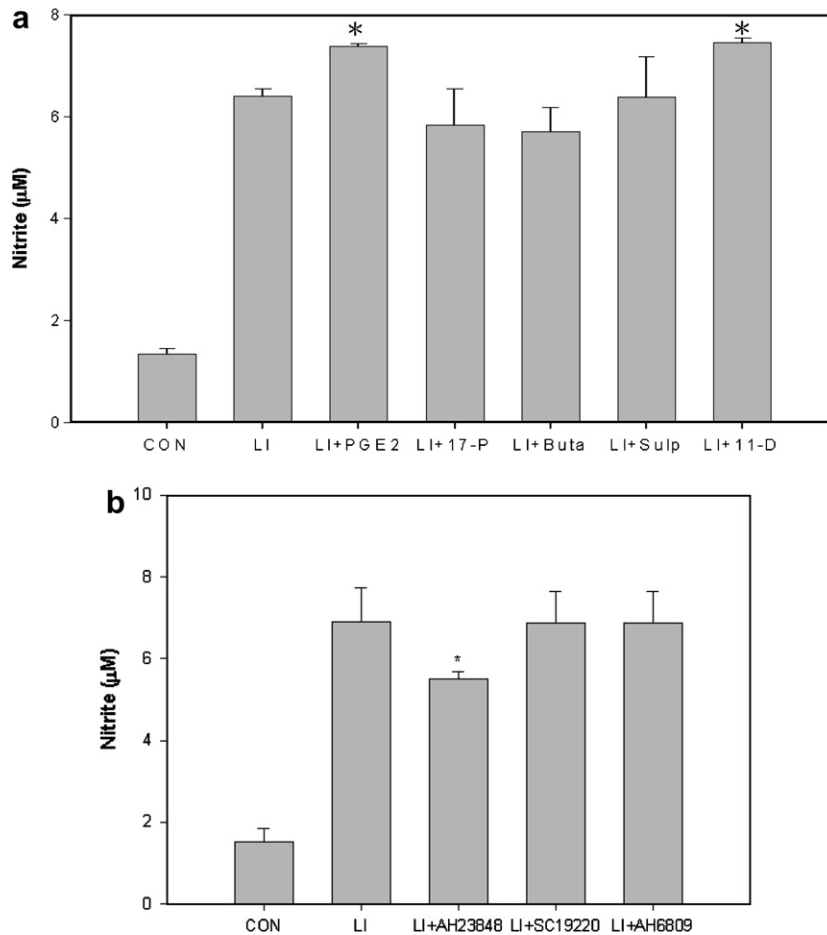


Fig. 2. (a) Effect of specific PGE₂ agonists on LPS + IFN γ -induced NO production in MES-13 cells. MES-13 cells grown in 6-well plates (approximately 0.8×10^5 cells/well) were treated with 1 μ g/ml LPS + 5 ng/ml IFN γ for 18 h in the presence of PGE₂ and specific agonists (11-deoxy-PGE₁, butaprost, sulprostone, or 17-phenyl trinor PGE₂ at a concentration of 1 μ M). The medium was collected for nitrite measurement. NO data are means \pm SEM values of three separate experiments, each done in triplicate. (b) Effect of specific PGE₂ antagonists on LPS + IFN γ -induced NO production in MES-13 cells. MES-13 cells grown in 6-well plates (approximately 0.8×10^5 cells/well) were treated with 1 μ g/ml LPS + 5 ng/ml IFN γ for 18 h in the presence of specific PGE₂ antagonists (AH23848, SC19220, and AH6809 at a concentration of 10 μ M). The medium was collected for nitrite measurement. NO data are means \pm SEM values of three separate experiments, each done in triplicate. * $p < 0.05$ compared to cells treated with LPS + IFN γ only. CON, control; LI, LPS + IFN γ ; 11-D, 11-deoxy-PGE₁; Buta, butaprost; Sulp, sulprostone; 17-P, 17-phenyl trinor PGE₂.

inhibitor significantly reduced the NO concentration and attenuated the iNOS mRNA and protein levels.

The EP4 receptor antagonist, AH23848, downregulated NO production through attenuation of cAMP signaling in MES-13 cells

As shown in Fig. 1b, the EP4 receptor utilized cAMP as a second messenger to transmit the signal of PGE₂ in MES-13 cells. To further confirm the role of cAMP in PGE₂-modulated NO synthesis in MES-13 cells, we examined the effect of cAMP on LPS + IFN γ -induced NO production. The NO concentration in the medium was measured in the presence of dibutyryl cAMP (db-cAMP), an analogue of cAMP. db-cAMP at 0.2 mM enhanced NO production from 6.4 ± 0.14 to 7.32 ± 0.08 μ mol/L (Fig. 3a). Moreover, co-supplementation of LPS + IFN γ with db-cAMP enhanced iNOS mRNA as shown in Fig. 3b. These observations demonstrated that the cAMP-mediated sig-

naling cascade is responsible for the role of PGE₂ in regulating iNOS activity in MES-13 cells. Moreover, endogenous cAMP levels in LPS + IFN γ -stimulated MES-13 cells were compared between AH23848-treated and -untreated groups. The endogenous cAMP level in LPS + IFN γ non-stimulated MES-13 cells (i.e., the control) was 385 ± 27 fmol/well containing 2.5×10^5 cells (Fig. 4). Stimulation of MES-13 cells with LPS + IFN γ for 18 h increased the endogenous cAMP level to 908 ± 26 fmol/well, while co-incubation of AH23848 with LPS + IFN γ decreased the endogenous cAMP level to 566 ± 32 fmol/well. These results indicate that through attenuation of cAMP signaling, AH23848 downregulated NO production in MES-13 cells.

AH23848-modulated iNOS protein stability

To determine whether AH23848 modulates iNOS protein stability, a pulse-chase experiment was performed

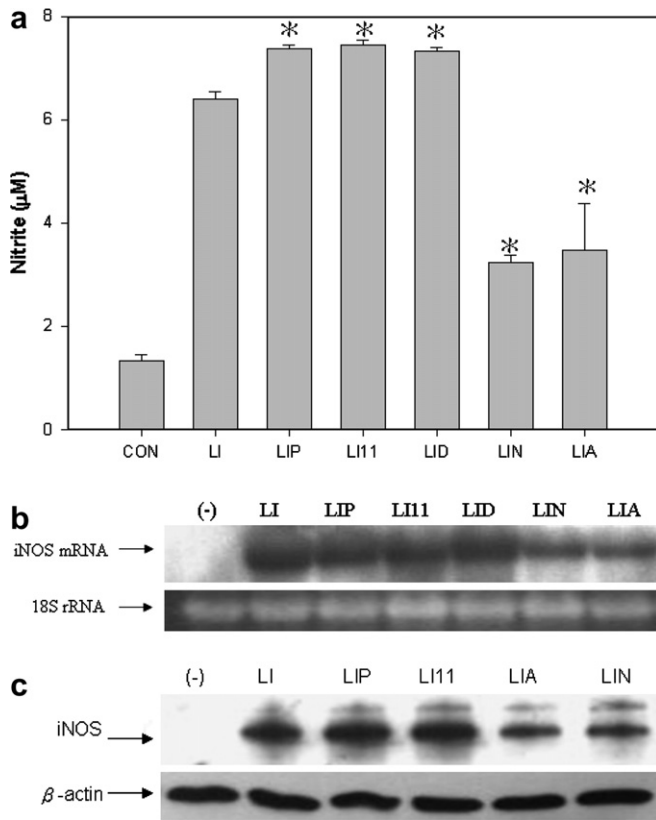


Fig. 3. (a) Effect of specific EP4 agonists and antagonists, cAMP analogue, a COX-2 specific inhibitor, on LPS + IFN γ -induced NO production in MES-13 cells. MES-13 cells grown in 6-well plates (approximately 0.8×10^5 cells/well) were treated with 1 μ g/ml LPS + 5 ng/ml IFN γ for 18 h in the presence of 1 μ M PGE $_2$, 1 μ M 11-deoxy PGE1, 0.2 mM dibutyl cAMP, 30 μ M AH23848, and 10 μ M NS398. The medium was collected for nitrite measurement. NO data are means \pm SEM values of three separate experiments, each done in triplicate. * $p < 0.05$ compared to cells treated with LPS + IFN γ only. (b) Effect of specific EP4 agonists and antagonists, cAMP analogue, a COX-2 specific inhibitor, on LPS + IFN γ -induced iNOS mRNA expression in MES-13 cells. For gene expression of iNOS, MES-13 cells (approximately 4×10^5 cells) were loaded on a 10-cm plate the day before the addition of 1 μ g/ml LPS + 5 ng/ml IFN γ in the presence of specific PGE $_2$ agonists and antagonists, cAMP analog and a COX-2 specific inhibitor. Following 18 h of stimulation, 20 μ g of total cellular RNA was purified and hybridized to a 32 P-labeled probe prepared from the RT-PCR product of the iNOS gene. To normalize the RNA amount of each sample, 28 S ribosomal RNA was used as an internal control. (c) Effect of specific EP4 agonists and antagonists and a COX-2 specific inhibitor on LPS + IFN γ -induced iNOS protein expression in MES-13 cells. MES-13 cells grown in 6-well plates (approximately 0.8×10^5 cells/well) were treated with 1 μ g/ml LPS + 5 ng/ml IFN γ for 18 h in the presence of specific PGE $_2$ agonists and antagonists and a COX-2 specific inhibitor. Following stimulation, 30 μ g of total cellular protein was purified and subjected to Western blot analysis using an iNOS antibody. β -Actin protein was used as an internal control. CON, -, control; LI, LPS + IFN γ ; LIP, LPS + IFN γ + PGE $_2$; LI11, LPS + IFN γ + 11-deoxy PGE1; LID, LPS + IFN γ + dibutyl cAMP; LIN, LPS + IFN γ + NS-398; LIA, LPS + IFN γ + AH23848.

(Fig. 5). MES-13 cells were treated with 1 μ g/ml LPS + 5 ng/ml IFN γ in the absence or presence of 30 μ M AH23848 for 18 h. The culture medium was then removed and replaced with starvation medium containing no methionine for 45 min. Pulse medium containing L-[35 S] methio-

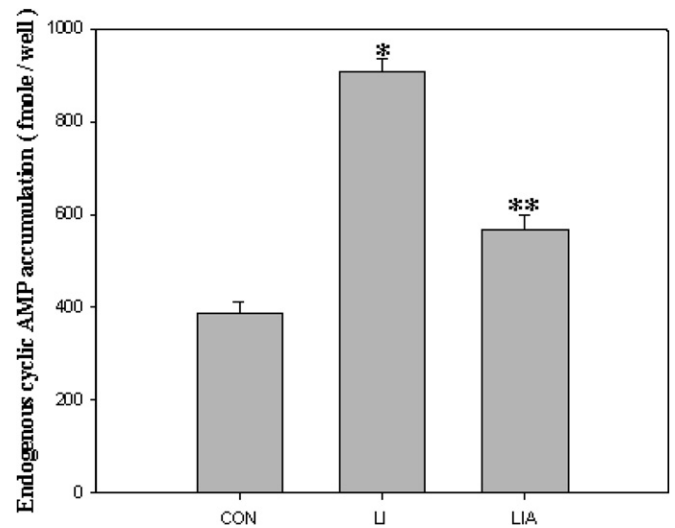


Fig. 4. AH23848 attenuated endogenous cAMP accumulation in MES-13 cells. MES-13 cells grown in 6-well plates (approximately 0.8×10^5 cells/well) were treated with 1 μ g/ml LPS + 5 ng/ml IFN γ in the absence or presence of 30 μ M AH23848 for 18 h. Cells from each treatment were washed with PBS and then preincubated in medium containing 0.5 mM IBMX for 10 min at 37 $^{\circ}$ C. PGE $_2$ was then added to the medium containing 0.5 mM IBMX and incubated at 37 $^{\circ}$ C for 10 min. Endogenous cAMP accumulation extracted from each well was quantified by a cAMP Biotrak enzyme immunoassay (EIA) system. The cAMP values are means \pm SD of triplicate assays from a representative of two similar experiments. * $p < 0.05$ compared to untreated MES-13 cells. ** $p < 0.05$ compared to cells treated with LPS + IFN γ .

nine (100 μ Ci/dish) was incubated with cells for 3 h followed by chase medium containing no labeled methionine. The cell lysate was then collected at the indicated time points (1, 3, and 6 h), and labeled iNOS protein was detected by immunoprecipitation, SDS-PAGE, and autoradiography. As shown in (Fig. 5), 78 \pm 8%, 60 \pm 3%, and 29 \pm 8% of L-[35 S] methionine-labeled iNOS proteins remained in AH23848-untreated MES-13 cells collected at 1, 3, and 6 h, respectively, while only 65 \pm 4%, 27 \pm 12%, and 9 \pm 9% of labeled iNOS proteins remained in AH23848-treated MES-13 cells collected in the same periods. These results revealed that iNOS proteins from AH23848-treated MES-13 cells decreased more rapidly than those of AH23848-untreated groups.

KT5720 inhibited NO production and iNOS protein expression through a decrease in iNOS protein stability

The role of PKA, the downstream signaling molecule of cAMP, in iNOS-stimulated NO synthesis was further investigated. The addition of 10 μ M H-89, 50 μ M H-8, and 1 μ M KT5720 attenuated LPS + IFN γ -induced NO production from 7.39 \pm 0.65 to 3.78 \pm 0.47, 1.04 \pm 0.38, and 3.31 \pm 0.55 μ mol/L, respectively (Fig. 6a). Moreover, the addition of H-89, H-8, and KT5720 diminished LPS + IFN γ -induced iNOS protein expression (Fig. 6b). There is no doubt as to the participation of PKA in the LPS + IFN γ -induced NO production in MES-13 cells.

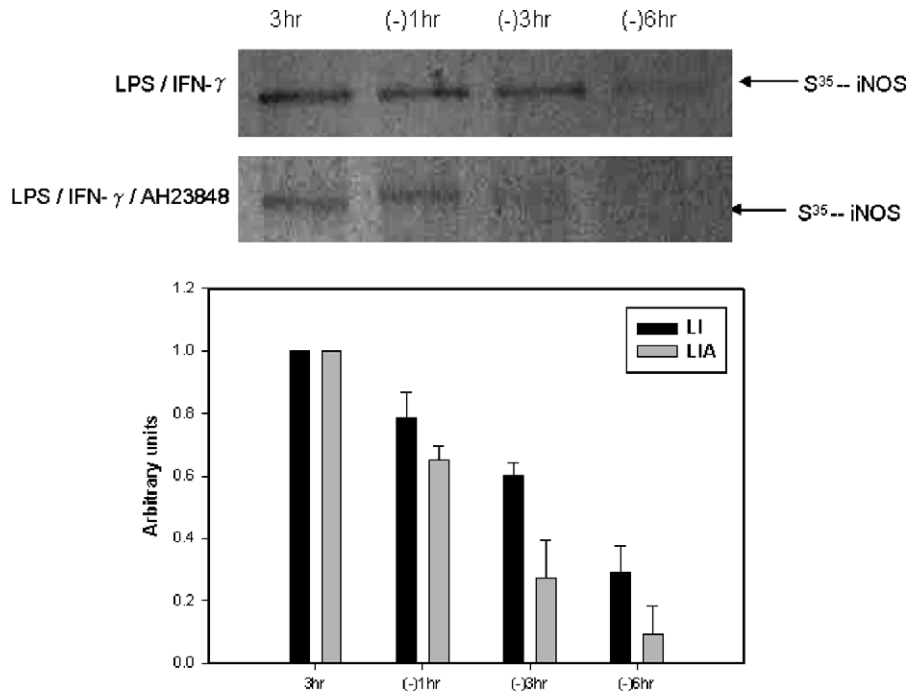


Fig. 5. AH23848 accelerated iNOS protein degradation in MES-13 cells as revealed by pulse-chase study. MES-13 cells grown in 10-cm plates (approximately 4×10^5 cells) were treated with $1 \mu\text{g/ml}$ LPS + 5 ng/ml IFN γ in the absence or presence of $30 \mu\text{M}$ AH23848 for 18 h. The culture medium was then removed and replaced with starvation medium containing no methionine for 45 min. Pulse medium containing L-[^{35}S] methionine ($100 \mu\text{Ci}$ per dish) was incubated with cells for 3 h followed by chase medium containing no labeled methionine. The cell lysate was then collected at the indicated time points (1, 3, and 6 h), and labeled iNOS protein was detected by immunoprecipitation, SDS-PAGE and autoradiography. The decrease in iNOS protein levels was expressed based on the control group (either AH23848-treated or -untreated LPS + IFN γ -stimulated cells after incubation with L-[^{35}S] methionine for 3 h), which were arbitrarily set to 1.

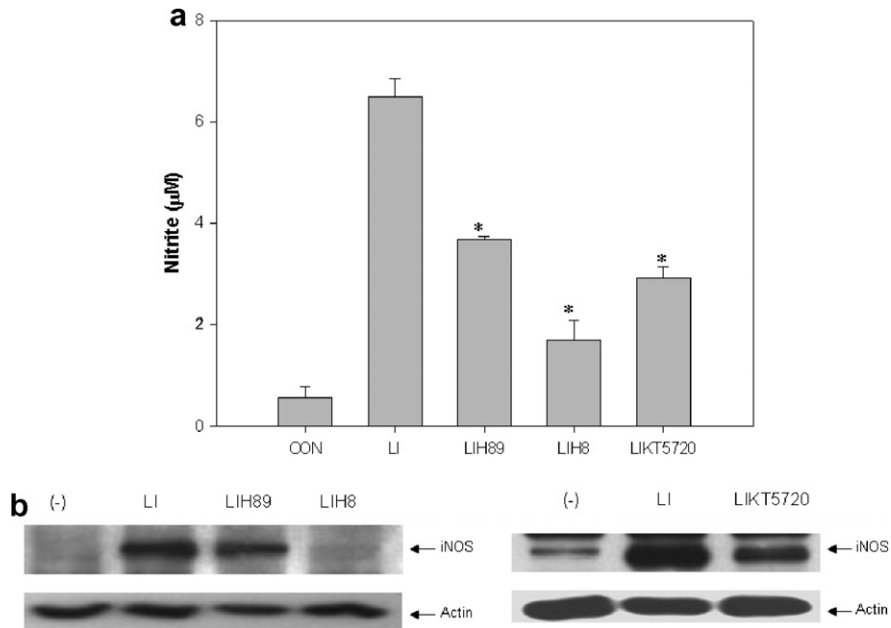


Fig. 6. Effect of PKA inhibitors on LPS + IFN γ -induced NO production and iNOS protein expression in MES-13 cells. (a) MES-13 cells grown in 6-well plates (approximately 0.8×10^5 cells/well) were treated with $1 \mu\text{g/ml}$ LPS + 5 ng/ml IFN γ for 18 h in the presence of PKA inhibitors ($10 \mu\text{M}$ H89, $50 \mu\text{M}$ H8, and $1 \mu\text{M}$ KT5720). The medium was collected for nitrite measurement. NO data are means \pm SEM values of three separate experiments, each done in triplicate. CON, control; LI, LPS + IFN γ ; LIH89, LPS + IFN γ + H89; LIKT5720, LPS + IFN γ + KT5720. (b) MES-13 cells grown in 6-well plates (approximately 0.8×10^5 cells/well) were treated with $1 \mu\text{g/ml}$ LPS + 5 ng/ml IFN γ for 18 h in the presence of PKA inhibitors ($10 \mu\text{M}$ H89, $50 \mu\text{M}$ H8, and $1 \mu\text{M}$ KT5720). Following stimulation, $30 \mu\text{g}$ of total cellular protein was purified and subjected to Western blot analysis using the iNOS antibody. β -Actin protein was used as an internal control.

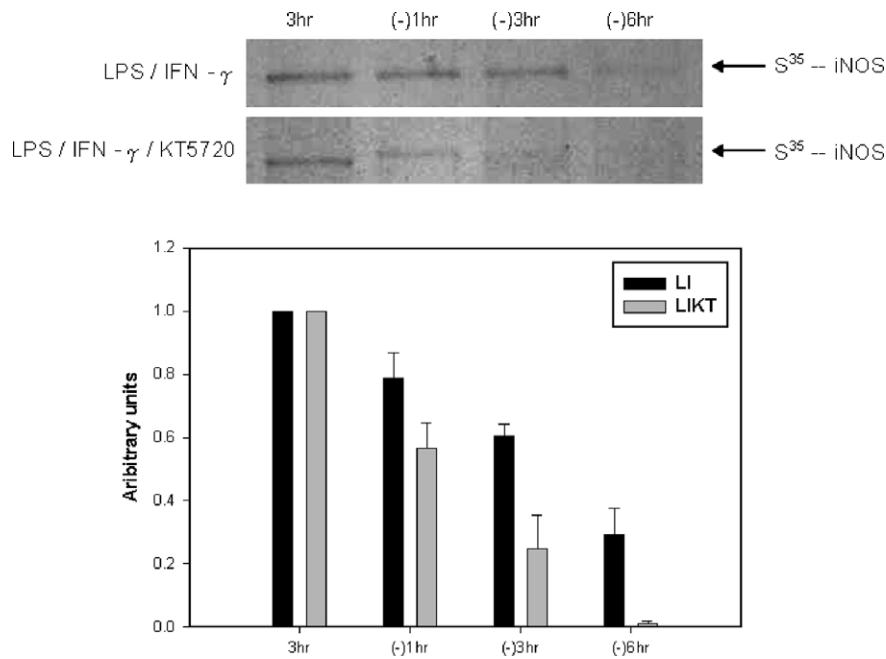


Fig. 7. KT5720 accelerated iNOS protein degradation in MES-13 cells as revealed by pulse-chase study. MES-13 cells grown in 10-cm plates (approximately 4×10^5 cells) were treated with 1 $\mu\text{g/ml}$ LPS + 5 ng/ml IFN γ in the absence or presence of 1 μM KT5720 for 18 h. The culture medium was then removed and replaced with starvation medium containing no L-methionine for 45 min. Pulse medium containing L-[^{35}S] methionine (100 μCi per dish) was incubated with cells for 3 h followed by chase medium containing no labeled methionine. The cell lysate was then collected at the indicated time points (1, 3, and 6 h), and the labeled iNOS protein was detected by immunoprecipitation, SDS-PAGE, and autoradiography. The decrease in iNOS protein levels was expressed based on the control group (either KT5720-treated or -untreated LPS + IFN γ -stimulated cells after incubation with L-[^{35}S] methionine for 3 h), which were arbitrarily set to 1.

Whether PKA modulates iNOS protein stability was further investigated by pulse-chase experiment. As shown in (Fig. 7), $78 \pm 8\%$, $60 \pm 3\%$, and $29 \pm 8\%$ of L-[^{35}S] methionine-labeled iNOS proteins remained in untreated MES-13 cells collected at 1, 3, and 6 h, respectively, while only $56 \pm 7\%$, $24 \pm 10\%$, and $1 \pm 0\%$ of L-[^{35}S] methionine-labeled iNOS proteins remained in KT5720-treated MES-13 cells. Taken together, these results indicate that iNOS proteins from KT5720-treated MES-13 cells decreased more rapidly than those of untreated groups.

Phosphatase inhibitors augmented iNOS activity in MES-13 cells

The effects of phosphatase inhibitors on iNOS activity were assessed by measuring the conversion of L-arginine into citrulline. MES-13 cells were stimulated with LPS + IFN γ for 16 h, followed by the addition of either a tyrosine phosphatase inhibitor (10 μM sodium orthovanadate) or a serine/threonine phosphatase inhibitor (20 nM okadaic acid) over a period of 15–120 min as indicated in Fig. 8. Total cellular proteins were collected, and the conversion of L-arginine into citrulline was measured. iNOS activities measured in the presence of LPS + IFN γ are presented as 100%. A short exposure of MES-13 cells to 10 μM sodium orthovanadate for 15 and 30 min increased the iNOS activity by about 10%. When the incubation times were prolonged to 60 and 120 min, a 30% increment

in iNOS activity was observed. For the effect of 20 nM okadaic acid, 25–30% augmentation of iNOS activity was also observed at 60 and 120 min of incubation. Thus, the phosphatase inhibitors augmented iNOS activity.

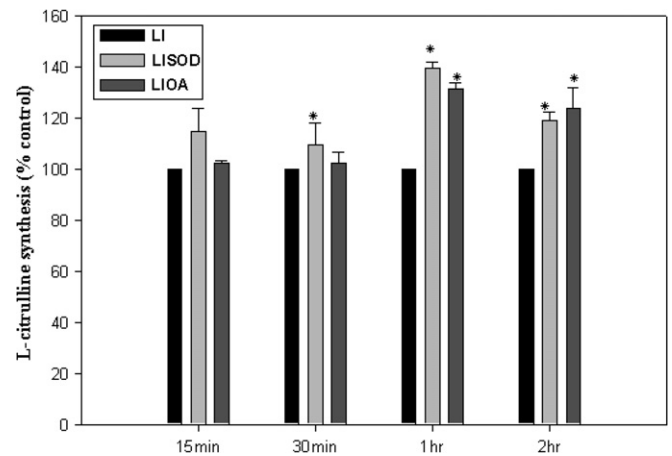


Fig. 8. Effects of phosphatase inhibitors on iNOS activity in MES-13 cells. MES-13 cells grown in 10-cm plates (approximately 4×10^5 cells/well) were treated with 1 $\mu\text{g/ml}$ LPS + 5 ng/ml IFN γ for 17.25, 17.5, 17, and 16 h, respectively. LPS and IFN γ were then completely removed from the culture medium. Fresh medium containing 10 μM sodium orthovanadate and 20 nM okadaic acid was added to the cells and incubated for further 15, 30, 60, and 120 min, respectively. After incubation, the total cell lysate was collected, and iNOS activity was measured. iNOS activities in the presence of LPS + IFN γ are presented as 100%. * $p < 0.05$ compared to cells treated with LPS + IFN γ for different incubation times.

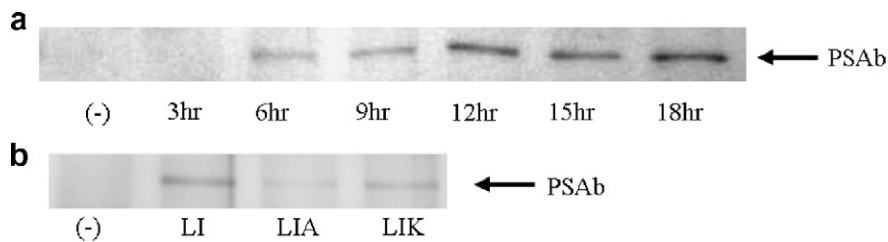


Fig. 9. The effect of AH23848 and KT5720 on serine/threonine phosphorylation of iNOS protein in activated MES-13 cells. (a) The immunoprecipitated iNOS protein recognized by PSAb in LPS + IFN γ -stimulated MES-13 cells over the 3–18 h period tested. (b) The protein intensity of iNOS recognized by the PSAb antibody in MES-13 cells treated with LPS + IFN γ only (lane 2) or co-supplied with either AH23848 (lane 3) or KT5720 (lane 4).

Effect of AH23848 and KT5720 on Ser/Thr phosphorylation of iNOS protein in activated MES-13 cells

The iNOS protein immunoprecipitated from LPS + IFN γ -treated MES-13 cells was recognized by PSAb, an antibody identifies substrate of PKA and other Arg-directed kinases but not non-phosphorylated substrate. The immunoprecipitated iNOS protein was recognized by PSAb in LPS + IFN γ -stimulated MES-13 cells over the 3–18 h period tested (Fig. 9a). Moreover, protein intensity of iNOS recognized by the PSAb antibody was reduced when MES-13 cells treated with LPS + IFN γ were co-supplied with either AH23848 or KT5720 (Fig. 9b). This indicated AH23848 and KT5720 attenuated serine/threonine phosphorylation of iNOS protein when the PGE₂-cAMP pathway was declined in activated MES-13 cells.

Discussion

Through EP4 receptors, PGE₂ modulates LPS + IFN γ -induced NO production in MES-13 cells. LPS + IFN γ -induced NO production was greatly inhibited by EP4 antagonist, but only slightly enhanced by exogenous EP4 agonist. This indicates that high endogenous PGE₂ levels in LPS + IFN γ -stimulated MES-13 cells might cause it to have a lower responsiveness toward exogenous PGE₂. Lin et al. [4] reported that the addition of exogenous PGE₂ enhanced LPS + IFN γ -induced NO production in J774 but not in Raw 264.7 cells, since the latter released a greater amount of endogenous PGE₂ than did J774. Our data support the notion that the differential effect of PGE₂ on NO induction might result from the difference in endogenous PGE₂ levels in a given cell type. Moreover, in MES-13 cells, attenuation of endogenous cAMP accumulation was observed when AH23848 was co-incubated with LPS + IFN γ . Attenuation of cAMP signaling in MES-13 cells may therefore account for the inhibitory effect of AH23848 toward LPS + IFN γ -induced NO production.

AH23848 significantly suppressed LPS + IFN γ -induced NO production and iNOS protein expression in a similar concentration-dependent manner. Conversely, as revealed by Northern blot analysis, the inhibitory effect of AH23848 on LPS + IFN γ -induced iNOS mRNA was not dose-dependently correlated (data not shown). These results led us to speculate that enhanced iNOS gene expres-

sion at the transcriptional level might not be the only approach through which the cAMP/PKA pathway can modulate iNOS-stimulated NO synthesis. This thought was supported by several studies, which demonstrated that cAMP could regulate NO synthesis via different mechanisms. For instance, either PGE₂ or elevation of intracellular cAMP inhibits NO production by upregulating arginase activity and depleting the availability of L-arginine [21,22]. Moreover, elevation of intracellular cAMP enhanced iNOS mRNA stability [23]. Although it is well documented that the promoter/enhancer regions of the iNOS gene contain binding sites for transcriptional factors activated by the cAMP/PKA pathway, one assessment should be mentioned that the cyclic AMP response element (CRE) has been located within the promoter region of the rat iNOS, but not in human or mouse iNOS [24]. However, despite the absence of the CRE, cAMP was able to enhance cytokine-induced iNOS activity in a murine astrocyte cell line [25]. One assumption suggests that cAMP might indirectly affect NO release through the reduced release of proinflammatory cytokines, such as TNF α [26]. Collectively, the differential effects of PGE₂/cAMP on NO induction may involve more intricate mechanisms.

As suggested by Won et al. [9], cAMP enhances iNOS protein expression by protecting the iNOS protein from degradation. This notion led to the following study to investigate whether cAMP plays a role in maintaining iNOS protein stability. Our data indicated that attenuation of cAMP signaling by AH23848 accelerated iNOS degradation as revealed by pulse-chase study. This indicated that reduction in intracellular cAMP level could lead to iNOS protein instability in MES-13 cells. A specific PKA inhibitor, KT5720, significantly inhibited LPS + IFN γ -induced NO production and iNOS protein expression in MES-13 cells. Pulse-chase study demonstrated that KT5720 accelerated iNOS degradation. This showed that activation of a downstream target of cAMP, i.e., PKA, is involved in maintaining iNOS protein stability. A short exposure of activated MES-13 cells to either okadaic acid or sodium orthovanadate augmented iNOS activity. Moreover, AH23848 and KT5720 decreased the signal recognized by PSAb, a phospho-(serine/threonine) PKA substrate antibody. This indicated the serine/threonine phosphorylation of iNOS protein was reduced when the EP4R-cAMP pathway was declined in activated MES-13 cells. Collectively,

these data suggested that iNOS-stimulated NO synthesis could be modulated through posttranslational modification of the iNOS protein. PKA may stabilize the iNOS protein through serine/threonine phosphorylation and maintain iNOS in a configuration facilitating NO synthesis, such as by exposing the active site for substrate binding. Although no information regarding this speculation is available for iNOS, a stable dimeric structure resisting neuronal NOS (nNOS) from proteolysis indicates that protein conformation is an important determinant of NOS stability [27]. Whether phosphorylation sustains the iNOS protein in a precise configuration required for dimer formation is unknown. Nonetheless, destabilization of the dimeric structure of nNOS triggers its degradation through a ubiquitin–proteasomal pathway suggesting that iNOS stability may be determined through a similar structural requirement. Although no direct evidence indicates a role of phosphorylation in protecting iNOS from degradation, an S714P mutant of iNOS, identified in Dahl/Rapp salt-sensitive rats, attenuated iNOS enzyme stability [28]. Accelerated ubiquitination and proteasome degradation of iNOS was found in an S714P mutant of iNOS [18]. Although the phosphorylation status of iNOS was unidentified in the S714P mutant, whether phosphorylation of iNOS protein protects the iNOS enzyme from degradation is certainly an interesting issue to be pursued in the future.

Numerous reports have demonstrated posttranslational modification of endothelial NOS and nNOS by protein kinases. However, only few papers described the posttranslational modification of iNOS by phosphorylation. Inhibition of tyrosine phosphatases by sodium orthovanadate increased the tyrosine phosphorylation of iNOS protein and its activity in Raw 264.7 murine macrophages [29]. Src-mediated phosphorylation of human iNOS caused a redistribution of its subcellular localization and attenuation of its catalytic activity [30]. Thus, posttranslational modification of iNOS by phosphorylation plays important roles in controlling the availability of the iNOS protein. Although one potential cAMP-dependent phosphorylation site has been displayed in the iNOS sequence [31], not much information regarding the phosphorylation of iNOS by PKA is available. Using Clustal W analysis, Butt et al. [32] performed multiple sequence alignments of different NOSs and identified putative PKA phosphorylation sites in human nNOS and eNOS, but not in iNOS. Thus, although our data demonstrated that the iNOS protein was recognized by PSAb in MES-13 cells, determining whether PKA directly phosphorylates iNOS and exerts an effect on its activity requires further analysis. Nevertheless, serine/threonine phosphorylation of iNOS has been identified in stimulated murine macrophages [33]. In vivo labeling studies from Salh et al. [34] revealed that the iNOS protein was phosphorylated, and abolishment of iNOS phosphorylation was associated with reduced NO production, which was correlated with the effects of LY294002, rapamycin, and wortmannin [34]. Thus, recognition of iNOS by PSAb may indicate a phosphorylation event of

iNOS by other Arg-directed kinases such as phosphatidylinositol 3-kinase (PI 3-K) instead of PKA merely.

In fact, cAMP/PKA signaling transactivates other signaling pathways. PKA may modulate iNOS activity through this transactivation. Stimulation of the EP4 receptor by PGE₂ results in activation of PI 3-K [35]. Activation of PI 3-K in modulating NO production occurred through a phosphorylation-dependent mechanism in RAW 264.7 cells [34]. Thus, it is reasonable to speculate that PGE₂–cAMP–PKA may modulate NO synthesis through phosphorylation of iNOS by PI 3-K. Moreover, phosphorylation of iNOS by tyrosine kinase regulates iNOS activity [29,30]. It is worthy of stressing that PKA interacts with Src signaling in the membrane microdomain [36]. Treatment of Rous sarcoma virus-transformed Chinese hamster ovary cells with cAMP increased phosphorylation of pp60src and its activity [37]. Activation of the C-terminal Src kinase (Csk) through a PGE₂–cAMP–PKA pathway inhibits Src activity [36]. Thus, another possibility is that PKA may transmit signaling to Src which in turn regulates iNOS activity. Whether PKA phosphorylates Src and mediates tyrosine phosphorylation of iNOS by Src should be examined in MES-13 cells in future studies.

In summary, AH23848, an EP4 antagonist, significantly suppressed LPS + IFN γ -induced NO production in MES-13 cells. Through attenuation of endogenous cAMP accumulation and a reduction in PKA signaling, AH23848 inhibited NO production via diminishing iNOS gene expression and accelerating iNOS protein degradation in MES-13 cells. Understanding the mechanism of regulating iNOS activity may provide a pharmacological strategy in treating glomerulonephritis.

Acknowledgment

This study was supported by a grant (NSC93-2320-B-040-053) from the National Science Council of the ROC.

References

- [1] A.G. Nicolson, N.E. Haites, N.G. McKay, H.M. Wilson, A.M. MacLeod, N. Benjamin, Induction of nitric oxide synthase in human mesangial cells, *Biochem. Biophys. Res. Commun.* 193 (1993) 1269–1274.
- [2] J. Pfeilschifter, Nitric oxide triggers the expression of proinflammatory and protective gene products in mesangial cells and the inflamed glomerulus, *Nephrol. Dial. Transplant.* 17 (2002) 347–348.
- [3] J.S. Goodwin, J. Ceuppens, Regulation of the immune response by prostaglandins, *J. Clin. Immunol.* 3 (1983) 295–315.
- [4] W.W. Lin, B.C. Chen, Y.W. Hsu, C.M. Lee, S.K. Shyue, Modulation of inducible nitric oxide synthase induction by prostaglandin E₂ in macrophages: distinct susceptibility in murine J774 and RAW 264.7 macrophages, *Prostaglandins Other Lipid Mediat.* 58 (1999) 87–101.
- [5] M.D. Breyer, R.M. Breyer, Prostaglandin E receptors and the kidney, *Am. J. Physiol. Renal Physiol.* 279 (2000) F12–F23.
- [6] T. Tetsuka, D. Daphna-Iken, S.K. Srivastava, L.D. Baier, J. DuMaine, A.R. Morrison, Cross-talk between cyclooxygenase and nitric oxide pathways: prostaglandin E₂ negatively modulates induction of nitric oxide synthase by interleukin 1, *Proc. Natl. Acad. Sci. USA* 91 (1994) 12168–12172.

- [7] D. Kunz, H. Muhl, G. Walker, J. Pfeilschifter, Two distinct signaling pathways trigger the expression of inducible nitric oxide synthase in rat renal mesangial cells, *Proc. Natl. Acad. Sci. USA* 91 (1994) 5387–5391.
- [8] A.V. Timoshenko, P.K. Lala, C. Chakraborty, PGE₂-mediated upregulation of iNOS in murine breast cancer cells through the activation of EP4 receptors, *Int. J. Cancer* 108 (2004) 384–389.
- [9] J.S. Won, Y.B. Im, A.K. Singh, I. Singh, Dual role of cAMP in iNOS expression in glial cells and macrophages is mediated by differential regulation of p38-MAPK/ATF-2 activation and iNOS stability, *Free Radic. Biol. Med.* 37 (2004) 1834–1844.
- [10] E. Galea, D.L. Feinstein, Regulation of the expression of the inflammatory nitric oxide synthase (NOS2) by cyclic AMP, *FASEB J.* 13 (1999) 2125–2137.
- [11] Z. Zidek, Role of cytokines in the modulation of nitric oxide production by cyclic AMP, *Eur. Cytokine Netw.* 12 (2001) 22–32.
- [12] D. Kunz, G. Walker, W. Eberhardt, J. Pfeilschifter, Molecular mechanisms of dexamethasone inhibition of nitric oxide synthase expression in interleukin 1 beta-stimulated mesangial cells: evidence for the involvement of transcriptional and posttranscriptional regulation, *Proc. Natl. Acad. Sci. USA* 93 (1996) 255–259.
- [13] T. Mitani, M. Terashima, H. Yoshimura, Y. Nariai, Y. Tanigawa, TGF-beta1 enhances degradation of IFN-gamma-induced iNOS protein via proteasomes in RAW 264.7 cells, *Nitric Oxide* 13 (2005) 78–87.
- [14] A. Musial, N.T. Eissa, Inducible nitric-oxide synthase is regulated by the proteasome degradation pathway, *J. Biol. Chem.* 276 (2001) 24268–24273.
- [15] G. Walker, J. Pfeilschifter, U. Otten, D. Kunz, Proteolytic cleavage of inducible nitric oxide synthase (iNOS) by calpain I, *Biochim. Biophys. Acta* 1568 (2001) 216–224.
- [16] E. Felley-Bosco, F.C. Bender, F. Courjault-Gautier, C. Bron, A.F. Quest, Caveolin-1 down-regulates inducible nitric oxide synthase via the proteasome pathway in human colon carcinoma cells, *Proc. Natl. Acad. Sci. USA* 97 (2000) 14334–14339.
- [17] M. Yoshida, Y. Xia, Heat shock protein 90 as an endogenous protein enhancer of inducible nitric-oxide synthase, *J. Biol. Chem.* 278 (2003) 36953–36958.
- [18] W.Z. Ying, P.W. Sanders, Accelerated ubiquitination and proteasome degradation of a genetic variant of inducible nitric oxide synthase, *Biochem. J.* 376 (2003) 789–794.
- [19] R. Nasrallah, O. Laneuville, S. Ferguson, R.L. Hebert, Effect of COX-2 inhibitor NS-398 on expression of PGE₂ receptor subtypes in M-1 mouse CCD cells, *Am. J. Physiol. Renal Physiol.* 281 (2001) F123–F132.
- [20] W.L. Cheng, C.K. Lii, H.W. Chen, T.H. Lin, K.L. Liu, Contribution of conjugated linoleic acid to the suppression of inflammatory responses through the regulation of the NF-kappaB pathway, *J. Agric. Food Chem.* 52 (2004) 71–78.
- [21] I.M. Corraliza, G. Soler, K. Eichmann, M. Modolell, Arginase induction by suppressors of nitric oxide synthesis (IL-4, IL-10 and PGE₂) in murine bone-marrow-derived macrophages, *Biochem. Biophys. Res. Commun.* 180 (1995) 667–673.
- [22] T. Gotoh, M. Mori, Arginase II downregulates nitric oxide (NO) production and prevents NO-mediated apoptosis in murine macrophage-derived RAW 264.7 cells, *J. Cell Biol.* 144 (1999) 427–434.
- [23] C.V. Oddis, R.L. Simmons, B.G. Hattler, M.S. Finkel, cAMP enhances inducible nitric oxide synthase mRNA stability in cardiac myocytes, *Am. J. Physiol.* 269 (1995) H2044–H2050.
- [24] W. Eberhardt, D. Kunz, R. Hummel, J. Pfeilschifter, Molecular cloning of the rat inducible nitric oxide synthase gene promoter, *Biochem. Biophys. Res. Commun.* 223 (1996) 752–756.
- [25] K.L. Burgher, J.A. Heroux, G.E. Ringheim, Cyclic AMP potentiation of cytokine-induced nitric oxide synthase activity in a murine astrocyte cell line, *Neurochem. Int.* 30 (1997) 483–489.
- [26] S.L. Kunkel, M. Spengler, M.A. May, R. Spengler, J. Larrick, D. Remick, Prostaglandin E₂ regulates macrophage-derived tumor necrosis factor gene expression, *J. Biol. Chem.* 263 (1988) 5380–5384.
- [27] A.Y. Dunbar, Y. Kamada, G.J. Jenkins, E.R. Lowe, S.S. Billecke, Y. Osawa, Ubiquitination and degradation of neuronal nitric-oxide synthase in vitro: dimer stabilization protects the enzyme from proteolysis, *Mol. Pharmacol.* 66 (2004) 964–969.
- [28] W.Z. Ying, H. Xia, P.W. Sanders, Nitric oxide synthase (NOS2) mutation in Dahl/Rapp rats decreases enzyme stability, *Circ. Res.* 89 (2001) 317–322.
- [29] J. Pan, K.L. Burgher, A.M. Szczepanik, G.E. Ringheim, Tyrosine phosphorylation of inducible nitric oxide synthase: implications for potential post-translational regulation, *Biochem. J.* 314 (1996) 889–894.
- [30] P. Hausel, H. Latado, F. Courjault-Gautier, E. Felley-Bosco, Src-mediated phosphorylation regulates subcellular distribution and activity of human inducible nitric oxide synthase, *Oncogene* 25 (2006) 198–206.
- [31] C.J. Lowenstein, C.S. Glatt, D.S. Bredt, S.H. Snyder, Cloned and expressed macrophage nitric oxide synthase contrasts with the brain enzyme, *Proc. Natl. Acad. Sci. USA* 89 (1992) 6711–6715.
- [32] E. Butt, M. Bernhardt, A. Smolenski, P. Kotsonis, L.G. Frohlich, A. Sickmann, H.E. Meyer, S.M. Lohmann, H.H. Schmidt, Endothelial nitric-oxide synthase (type III) is activated and becomes calcium independent upon phosphorylation by cyclic nucleotide-dependent protein kinases, *J. Biol. Chem.* 275 (2000) 5179–5187.
- [33] Y. Vodovotz, D. Russell, Q.W. Xie, C. Bogdan, C. Nathan, Vesicle membrane association of nitric oxide synthase in primary mouse macrophages, *J. Immunol.* 154 (1995) 2914–2925.
- [34] B. Salh, R. Wagey, A. Marotta, J.S. Tao, S. Pelech, Activation of phosphatidylinositol 3-kinase, protein kinase B, and p70 S6 kinases in lipopolysaccharide-stimulated Raw 264.7 cells: differential effects of rapamycin, Ly294002, and wortmannin on nitric oxide production, *J. Immunol.* 161 (1998) 6947–6954.
- [35] H. Fujino, S. Salvi, J.W. Regan, Differential regulation of phosphorylation of the cAMP response element-binding protein after activation of EP2 and EP4 prostanoid receptors by prostaglandin E₂, *Mol. Pharmacol.* 68 (2005) 251–259.
- [36] H. Abrahamsen, T. Vang, K. Tasken, Protein kinase A intersects SRC signaling in membrane microdomains, *J. Biol. Chem.* 278 (2003) 17170–17177.
- [37] C.W. Roth, N.D. Richert, I. Pastan, M.M. Gottesman, Cyclic AMP treatment of Rous sarcoma virus-transformed Chinese hamster ovary cells increases phosphorylation of pp60src and increases pp60src kinase activity, *J. Biol. Chem.* 258 (1983) 10768–10773.